ARMY RESEARCH LABORATORY

SBS Suppression and Coherent Combination of Fiber MOPAs via Chirped Diode Lasers Final Report

by Jeffrey O. White

ARL-TR-6945 May 2014

NOTICES

Disclaimers

The findings in this report are not to be construed as an official Department of the Army position unless so designated by other authorized documents.

Citation of manufacturer's or trade names does not constitute an official endorsement or approval of the use thereof.

Destroy this report when it is no longer needed. Do not return it to the originator.

Army Research Laboratory
Adelphi, MD 20783-1197

ARL-TR-6945 **May 2014**

SBS Suppression and Coherent Combination of Fiber MOPAs via Chirped Diode Lasers Final Report

Jeffrey O. White
Sensors and Electron Devices Directorate, ARL

REPORT DOCUMENTATION PAGE

Form Approved
OMB No. 0704-0188

PLEASE DO NOT RETURN YOUR FORM TO THE ABOVE ADDRESS.

1. REPORT DATE *(DD-MM-YYYY)*	**2. REPORT TYPE**	**3. DATES COVERED (From - To)**
May 2014	Final	March 2011 to February 2014

4. TITLE AND SUBTITLE
SBS Suppression and Coherent Combination of Fiber MOPAs via Chirped Diode Lasers Final Report

5a. CONTRACT NUMBER
11-SA-0405

5b. GRANT NUMBER

5c. PROGRAM ELEMENT NUMBER
622120

6. AUTHOR(S)
Jeffrey O. White

5d. PROJECT NUMBER

5e. TASK NUMBER

5f. WORK UNIT NUMBER

7. PERFORMING ORGANIZATION NAME(S) AND ADDRESS(ES)
U.S. Army Research Laboratory
RDRL-SEE-M
2800 Powder Mill Road
Adelphi, MD 20783-1197

8. PERFORMING ORGANIZATION REPORT NUMBER
ARL-TR-6945

9. SPONSORING/MONITORING AGENCY NAME(S) AND ADDRESS(ES)
High Energy Laser Joint Technology Office
801 University Blvd. SE, Suite 209, Albuquerque, NM 87106

10. SPONSOR/MONITOR'S ACRONYM(S)
HEL-JTO

11. SPONSOR/MONITOR'S REPORT NUMBER(S)

12. DISTRIBUTION/AVAILABILITY STATEMENT
Approved for public release; distribution unlimited.

13. SUPPLEMENTARY NOTES

14. ABSTRACT
This is the final report for a High Energy Laser Joint Technology Office (HEL-JTO) contract to investigate the use of a chirped seed laser to suppress stimulated Brillouin scattering (SBS) in high power fiber amplifiers. Both experimental and theoretical results are described. The conventional way of suppressing SBS shortens the coherence length of the laser output to the point where coherently combining multiple amplifiers requires carefully matching the amplifier path lengths. The method we report on here has the advantage of allowing coherent combination without strict path length matching. Another disadvantage of the conventional method of suppressing SBS is that the threshold decreases as 1/L, where L is the length of the delivery fiber. The advantage of a chirped seed laser is that the SBS threshold decreases slower than 1/L and is almost independent of L in the limit of long fibers and high chirps.

15. SUBJECT TERMS
fiber lasers, stimulated Brillouin scattering, coherent combination

16. SECURITY CLASSIFICATION OF:			**17. LIMITATION OF ABSTRACT**	**18. NUMBER OF PAGES**	**19a. NAME OF RESPONSIBLE PERSON**
a. REPORT	**b. ABSTRACT**	**c. THIS PAGE**			Jeffrey O. White
Unclassified	Unclassified	Unclassified	UU	28	**19b. TELEPHONE NUMBER** (*Include area code*) (301) 394-0069

Standard Form 298 (Rev. 8/98)
Prescribed by ANSI Std. Z39.18

Contents

List of Figures

Acknowledgments

Many colleagues participated in the execution of this contract. The chirped seed was developed by Naresh Satyan, Arseny Vasilyev, George Rakuljic, and Amnon Yariv. Their work was supported by U.S. Army Research Office (ARO) under grant W911NF-11-2-0081. The initial SBS suppression experiments at 1.5 μm were done by Olukayode Okusaga, James P. Cahill, and me. The adiabatic model was developed by me. The dynamic model of a passive fiber was developed by Carl Mungan and me, with help from Steven Rogers and Naresh Satyan. The coherent combination at 1.5 μm was carried out by Eliot Petersen, with help from Arseny Vasilyev, Naresh Satyan, and Zhi Yi Yang. The dynamic model of an active/passive fiber was developed by Eliot Petersen and me, with help from Zhi Yi Yang. The 300 W YbFA experiments, and the coherent combination at 20 W was carried out by Eliot Petersen with help from Zhi Yi Yang. The 600 W YbFA experiments were carried out at Nufern by John Edgecumbe, Eliot Petersen, and me. The multi-mode instability analysis was done by me.

1. Introduction

Fiber lasers have become leading candidates for defending against unmanned aerial vehicles, rockets, artillery shells, mortar rounds, and missiles. This is because of their high electrical-to-optical efficiency, high beam quality, and ruggedness, and because multi-kilowatt output powers are now commercially available (*1*). Laser output on the order of 100 kW would enable the harder targets to be defeated at longer distances. At present, reaching this power level requires combining multiple fiber amplifiers in parallel, either in an incoherent or coherent fashion (*2*). This report concerns the latter, which is best suited for a tiled aperture geometry, which has the major advantage of being able to pre-distort the emitted wavefront so as to compensate for propagation through atmospheric turbulence.

2. Experiments and Modeling of SBS Suppression in Passive Fiber at 1.5 µ

Our first model of simulated Brillouin scattering (SBS) with a chirped seed was adiabatic in the sense that it should be valid for chirps less than the Brillouin bandwidth (~100 MHz) squared, i.e., 10^{16} Hz/s. In this case, a phonon, during its lifetime, would not see the laser frequency change by a large fraction of the Brillouin linewidth. This model (*3*) indicated that chirping the seed at 10^{16} Hz/s, close to that which had already been achieved with a diode laser, would raise the threshold for SBS by a factor of 35 for a passive ~17.5 m fiber (figure 1). This fiber length corresponds to the 15 m final stage in the IPG 10 kW amplifier, plus a 2 m delivery fiber, both with a core diameter of 27.5 µm. The Brillouin gain was taken to be 0.24 cm/GW, based on recent measurements (*4*). The results show a threshold that is independent of chirp below 10^{13} Hz/s and rises linearly with chirp at higher chirp values.

The (spontaneous) Brillouin linewidth for these calculations was taken to be 20 MHz, a conservative estimate based on the 16 MHz linewidth consistent with the known 10 ns phonon lifetime in fused silica. Later, in our own measurements on actual large mode area (LMA) fibers, we found that the Brillouin linewidth was closer to 120 MHz. Together with the effect of gain due to the inversion in an amplifier, this meant that suppressing SBS would require chirps at least 10 times faster than we anticipated.

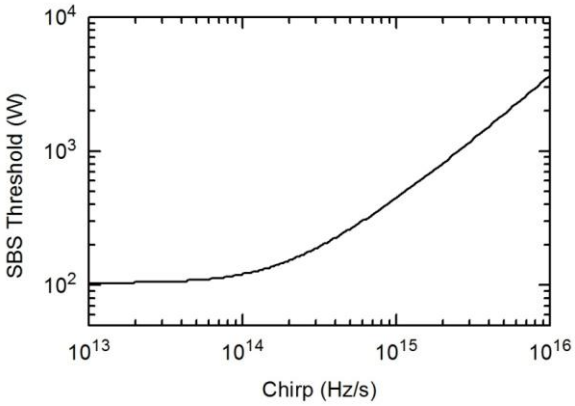

Figure 1. SBS threshold vs. chirp, for a passive 17.5 m fiber with 27.5 μm core, $\Delta\nu_B = 20$ MHz.

The chirped seed is based on a vertical cavity surface emitting diode laser in an opto-electronic feedback circuit (*5*) (figure 2). The first seed we tested had a maximum chirp of 5×10^{15} Hz/s, obtained by sweeping 500 GHz (4 nm at 1.55 μm) in 100 μs. The initial experiments (*3*) were performed at 1.55 μm with a long 6 km single mode fiber (mode field diameter 8 μm) because we could amplify the seed to only ~5 W.* The symbols in figure 3 represent the experimental data; the solid curves are solutions of the equations in (*3*). Using an optical spectrum analyzer, we determined the ratio of Brillouin to Rayleigh backscattering is $P_B/P_R = 1.5 \times 10^{-2}$ below threshold. The value of $g_0 = 2.5 \times 10^{-12}$ m/W was chosen to fit the zero-chirp data. The Brillouin linewidth $\Delta\nu_B = 110$ MHz was chosen to fit the low chirp data.

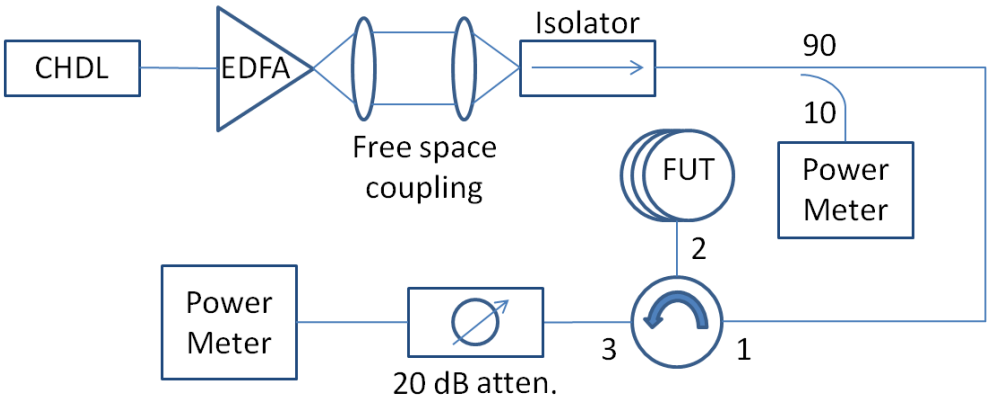

Figure 2. Experimental setup for measuring SBS suppression. CHDL is the chirped diode laser. FUT is the fiber under test.

*We used a dispersion-shifted Corning fiber, only because its Brillouin spectrum has ony a single peak. More recent fibers, e.g., SMF28e+, have an inner and outer core with different sound velocities, and thus two distinct Brillouin peaks. The purpose is to raise the SBS threshold by a factor of two. For us, a double peak would just make the data analysis more difficult.

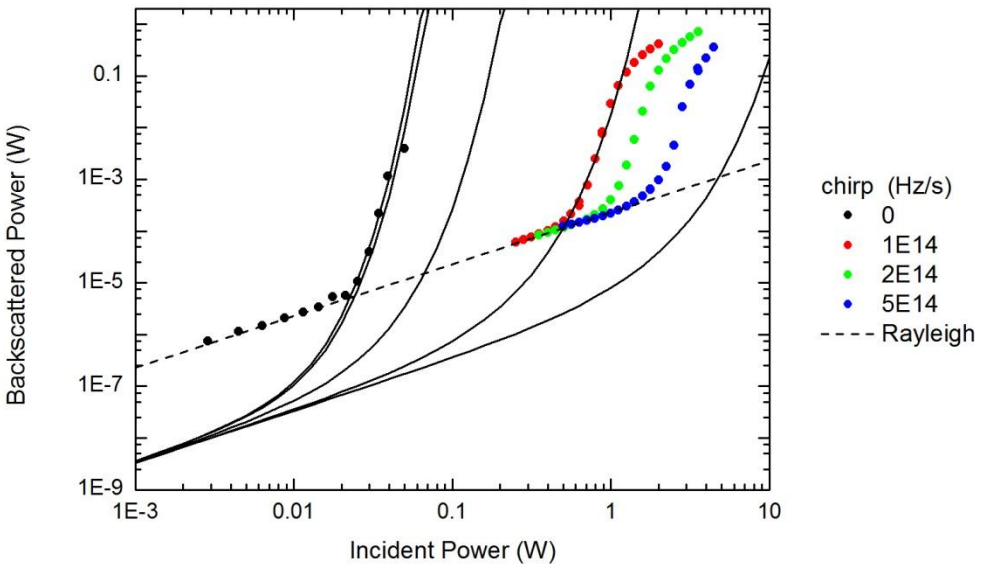

Figure 3. Backscattered power vs incident power for a 6-km dispersion-shifted fiber having a mode field diameter of 8 μm. The symbols are the experimental data taken at chirps of β=0, 10^{14}, 2×10^{14}, and 5×10^{14} Hz/s. The curves are calculations of the backscattered Brillouin power for β=10^{11} – 10^{15} Hz/s (left to right). The dashed line is the backscattered Rayleigh power.

Using a self-heterodyne technique (*4*), we made an independent high-resolution measurement of $\Delta\nu_B$, which allowed us to separate the Rayleigh and Brillouin components. We made sure to remain within the spontaneous regime. The Brillouin spectrum in this single mode fiber has a width of 39 MHz, comparable to other recent measurements at 1.5 μm (*4*).

During the first year, we also developed a dynamic model of SBS, which should be accurate to higher chirps (*6*). Instead of injecting a weak Stokes seed at $z = L$, the SBS builds up from spontaneous emission along the entire length of the fiber. The spontaneous emission is described by including a Langevin noise term in the rate equation for the amplitude of the acoustic wave. The results again showed a linear increase in SBS threshold with chirp. As an example, figure 4 shows results from the dynamic model (black squares) and the adiabatic model (red curve) of a 17.5 m fiber, with a core diameter of 27.5 μm, a Brillouin linewidth of 20 MHz, and a Brillouin gain of $g_0 = 1.2 \times 10^{-11}$ m/W.

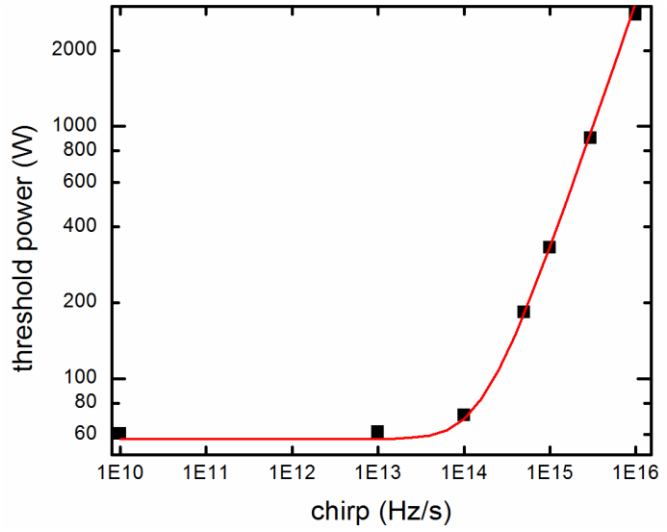

Figure 4. Threshold power vs chirp for a fiber with the specifications given in the text. The black squares are the dynamic model, the red line is the adiabatic model.

3. Pulsed Experiments and Modeling of an Amplifier at 1.5 µm

To determine how the SBS suppression operated at higher powers, and in active fibers, we undertook an experiment with a four-stage pulsed ErFA at Fibertek (figure 5). In this case, the power entering the final stage was kept constant, while the current to the pump diodes was changed to vary the amplifier output power. The pulse length is ~1 µs and the repetition rate is 10 kHz.

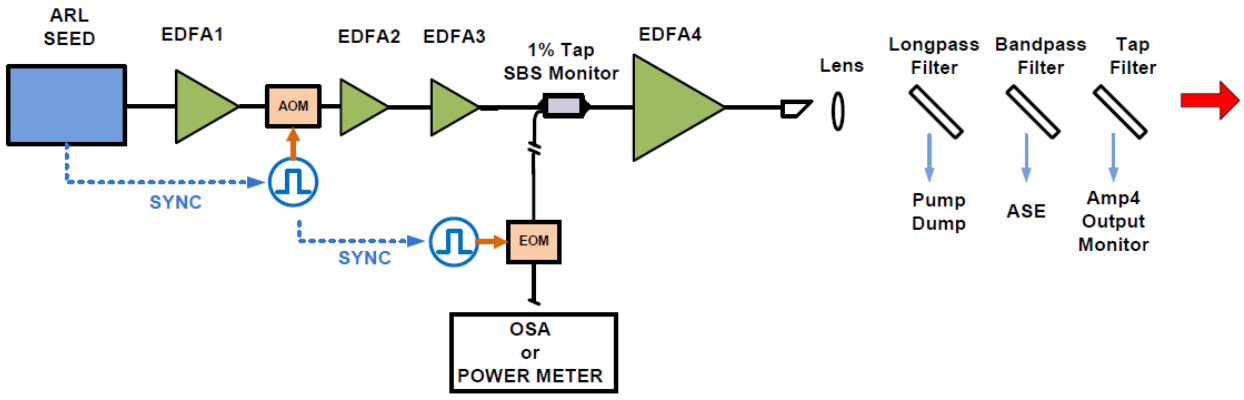

Figure 5. Experimental setup for seeding the pulsed 1.5 µ amplifier at Fibertek.

At zero chirp with the 18 m fiber and 5.6 µJ of output, the backscattered spectrum (figure 6) shows a Rayleigh peak and a Brillouin peak of approximately equal height, which is our definition of threshold for this experiment. The peak widths are instrument-limited. The Stokes

shift at this wavelength is 0.083 nm. At 7.6 µJ output—i.e., 50% above threshold—the SBS power increases by a factor of 7.5, illustrating the problem.

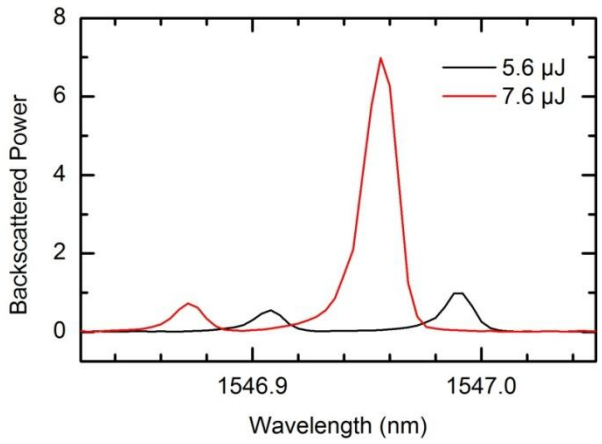

Figure 6. Backscattered spectrum at zero chirp with the 18 m amplifier operating at SBS threshold and above threshold.

The results show that the 5 µJ threshold with no chirp increased to 50 µJ at a chirp of 5×1015 Hz/s. This is in good agreement with a time-dependent model (*7*). The 80 µJ output corresponds to a peak power of ~80 W. Tests were also made up to 250 W by shortening the fiber to 12 m, which is closer to the optimum length for this amplifier. The results were similar, although for shorter fibers, the SBS suppression is less dramatic for a given chirp.

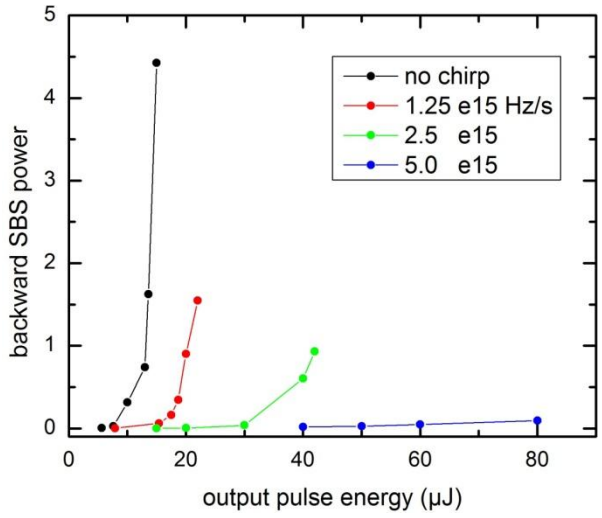

Figure 7. Backward SBS power vs output pulse energy for the 18 m amplifier.

4. Coherent Combining of a Chirped Seed Er Fiber Amplifier at 1.55 µm

In recent work on coherent combining of fiber amplifiers, path length matching has been achieved by using a variable delay line and an electro-optic phase shifter (*8*). A fiber stretcher can also compensate for ~3 mm of path length difference with a frequency response of ~1 kHz. An important advantage of using a linearly chirped seed is its long effective coherence length, particularly for combining multiple amplifiers with different path lengths. By shifting the frequency of the seed entering each amplifier by an amount proportional to the difference in path length, relative to a reference leg, the amplifier outputs can be made to have the same frequency and be in phase (*9*).

The frequency shifting is accomplished via a free-space acousto-optic device, with fiber pigtails. The shifter is driven by a heterodyne phase-locked loop circuit, with input from a photodiode that monitors the interference between the reference and a sample of the amplifier output (figure 8). The heterodyne frequency is 100 MHz, corresponding to the nominal frequency shift of our device (*10*). At 90 and 100 MHz, the throughput is down by ~3 dB. Each phase-locked loop has a digitally synthesized local oscillator; all are synchronized by a master clock. The relative phase of each output beam can be adjusted at the start of each scan.

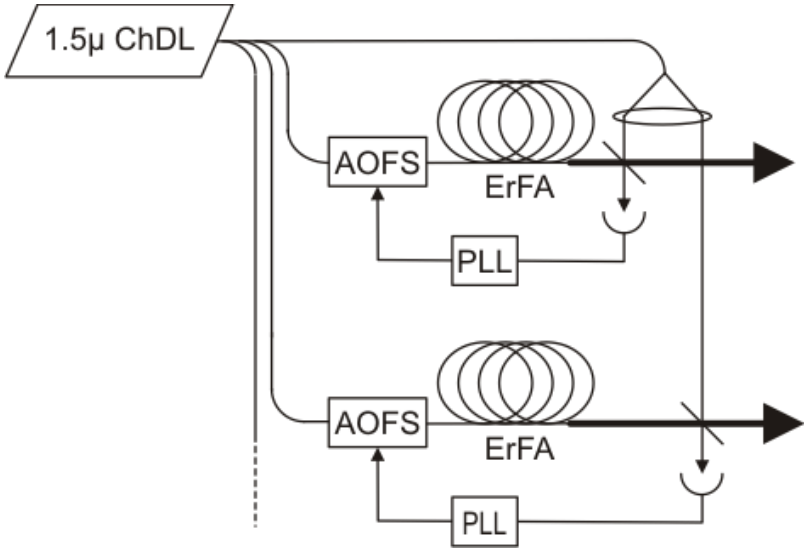

Figure 8. Apparatus for coherently combining the output of two ErFAs.

The coherent combining was tested with two ErFAs (*11*). The coherence was verified by overlapping the two amplifier outputs in the focal plane of a lens and imaging the fringes, and by doing an I/Q demodulation of the electrical signal coming from each photodiode. The far-field intensity profiles of channel A and B are Gaussian (figure 9). When the two channels are combined in phase, the spot size in the horizontal direction decreases, and side lobes appear, due

to the less-than-unity fill factor in the near-field. Horizontal cross-sections show that the on-axis intensity increases by a factor of three, as opposed to the theoretical factor of four. An efficiency of less than 100% can be due to differences in spot size, wavefront, and polarization, as well as a less-than-perfect coherence. Another contribution comes from the interval, at the end of a sweep, during which the PLL has to relock.

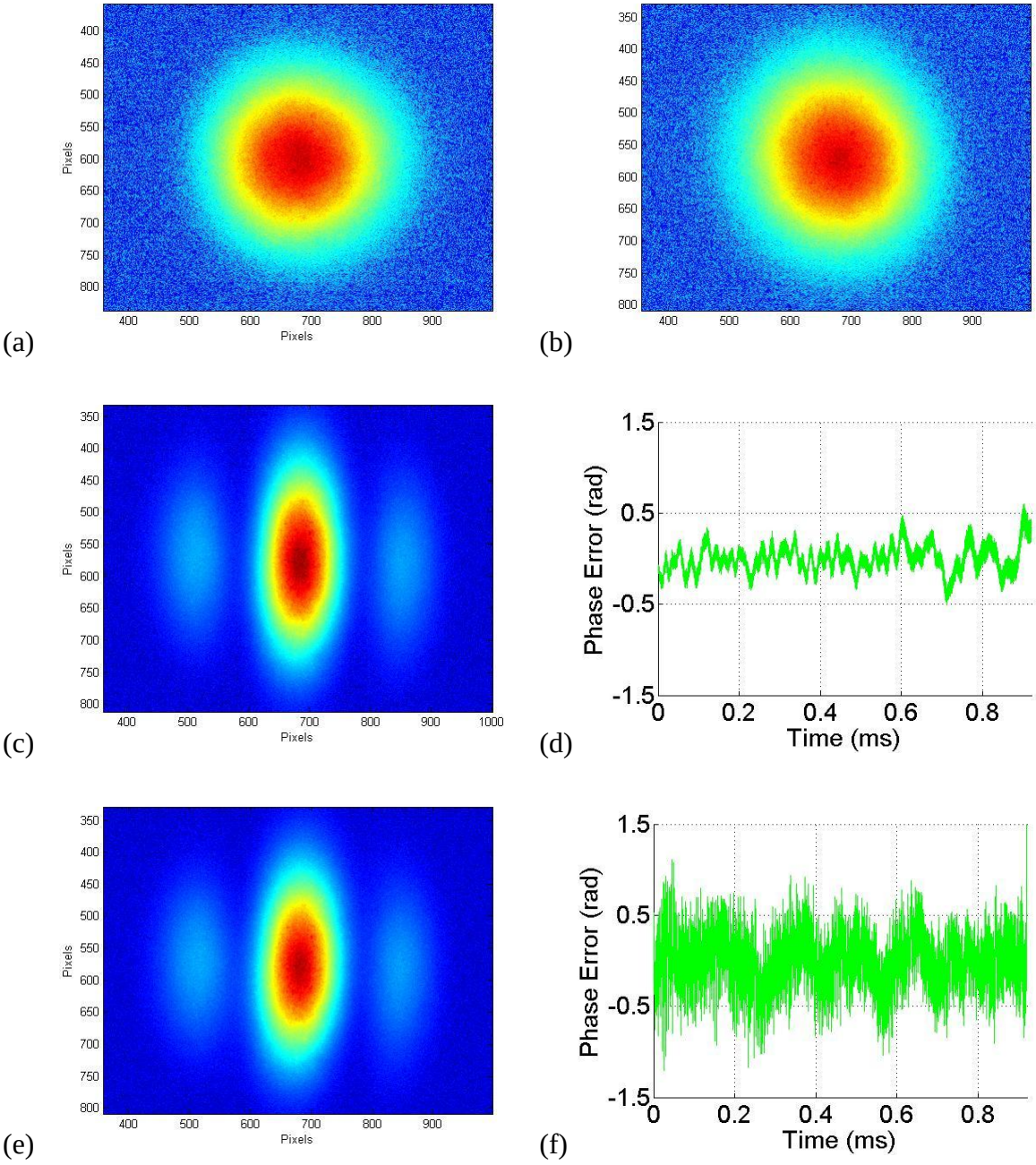

Figure 9. (a, b) far-field intensity profiles of channels A and B alone. (c, d) Far-field intensity and relative phase error when both channels are present, for a pathlength mismatch of 1.8 cm. (e, f) For a mismatch of 34 cm.

The phase error obtained from the time-resolved photodiode current, if measured away from the reset transients, shows the contribution due to only the nonlinearity of the chirp and the finite bandwidth of the phase-locked loop. According to the formula

$$\eta_{cc} = 1 - \frac{N-1}{N}\sigma_\phi^2$$

the coherent combining efficiency would be 99.0% at a pathlength difference of 1.8 cm, and 96.4% at 34 cm. For large N, these efficiencies would decrease to 98% and 92.8%, respectively.

5. Experiments and Modeling of SBS Suppression in an Active Fiber at 1.06 μ

The second chirped laser we tested has a wavelength of 1.06 μ, suitable for seeding a ytterbium fiber amplifier (YbFA). Initial tests were performed on a 40-W YbFA with a 40-m delivery fiber and a 400-W YbFA with a 2-m delivery fiber (figure 10). MATLAB code was written to simulate SBS during chirped seed amplification and subsequent delivery through a passive fiber (*12*). The code was validated with the results from both experiments.

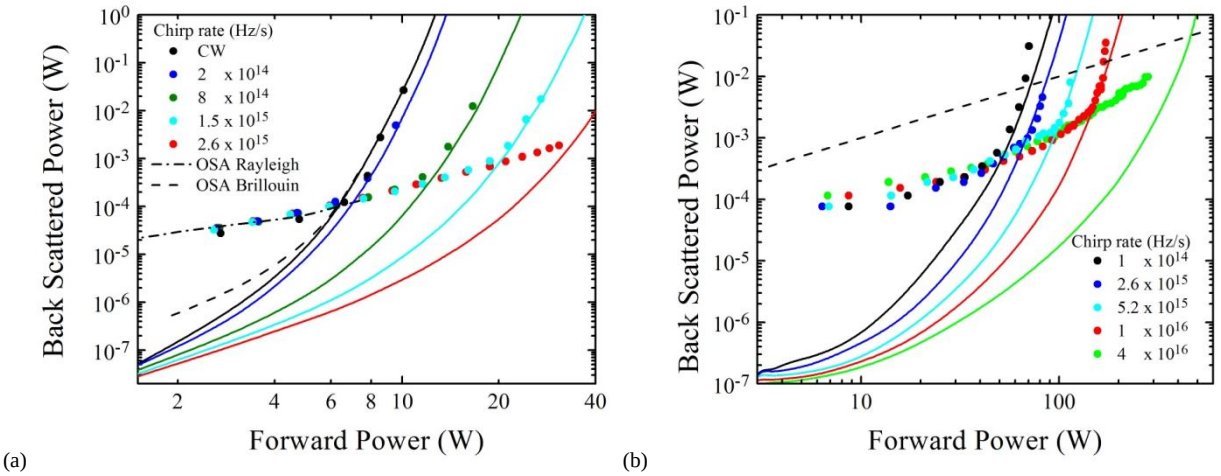

Figure 10. (a) Backscattered power vs forward power for various chirps, for a 5 m active fiber and a 41.5 m delivery fiber, both PM. The points are experimental data; the solid lines are results of the simulation. The dashed (Brillouin) and dash-dot (Rayleigh) lines are measured at zero chirp with an optical spectrum analyzer. (b) Results from a different amplifier with a 10 m active fiber and 2 m delivery fiber, both non-PM.

After validation, the code was used to extrapolate to faster chirps and higher powers, using the same values of Brillouin gain and bandwidth. The results were used to generate operating curves that show what chirp would be required to obtain a given amplifier output power transmitted through a given delivery fiber (figure 11). The parameters used are a 10-m active fiber of

core/cladding diameter 25/400 μ. Note that the threshold decreases slower than 1/L and at high chirps, and long fibers appear to be becoming independent of fiber length.

Also shown for comparison is the threshold for a seed broadened to a 26 GHz FWHM via a random phase modulation. Note that the threshold in this case decreases faster than 1/L, as shown by the dashed line. This illustrates a major advantage of chirped seed amplification relative to the conventional method of broadening a seed via random phase modulation.

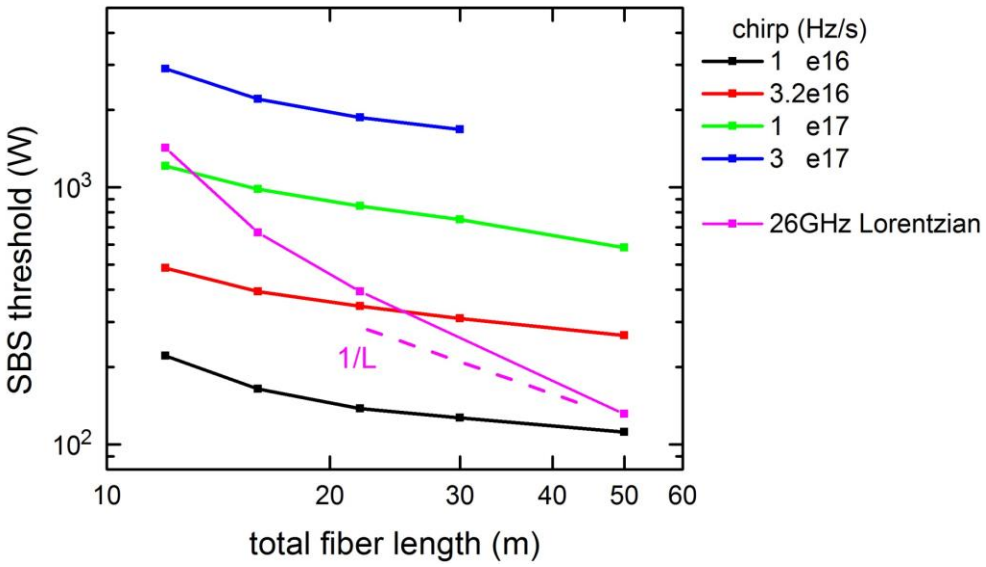

Figure 11. Operating curves for chirped seed amplification.

Not shown explicitly in the above experimental data is the fact that SBS pops up when the chirp of the seed laser changes direction. This happens whether the frequency vs. time waveform is a triangular wave or a sawtooth. With a photodiode and an oscilloscope, one can easily avoid the SBS by taking data away from the reset interval; however, the interlocks are designed to turn off the amplifiers when even a short pulse of SBS propagates backwards out of the final stage.

To circumvent the problem, we injected a square pulse of broadband light from a superluminescent laser diode (*13*) at the turning points. This technique allowed us to obtain some preliminary data with a higher power amplifier at Nufern, but SBS continued to pop up at the transition point between the SDL and the ChDL, for reasons that we did not understand at the time. The technique had the additional practical disadvantage that the coherence length of the SDL is far too short for coherent combining.

The next approach was to operate two ChDLs, chirping in opposite directions. One can avoid the periodic points where the chirp goes to zero by switching from one seed to the other at the appropriate time, so that the light injected into the amplifier is always chirping at full speed. The outputs from the two synchronized sources were connected to the inputs of a 2 × 1 bulk $LiNbO_3$ electro-optic switch (*14*) so that the even sweeps came from one laser and the odd sweeps from the other (figure 12). The transition was timed to occur just before each laser reached the top (or

bottom) of its scan. The 10–90% spec on the switch is <0.1 µs. Faster switches are available, based on $LiNbO_3$ waveguides, but they suffer from optical damage at the mW power levels produced by our seed laser. The synchronization of the two sources is selectable by the user so that the frequency waveform transmitted by the switch is either (a) a negative sawtooth, (b) a positive sawtooth, or (c) a triangle wave.

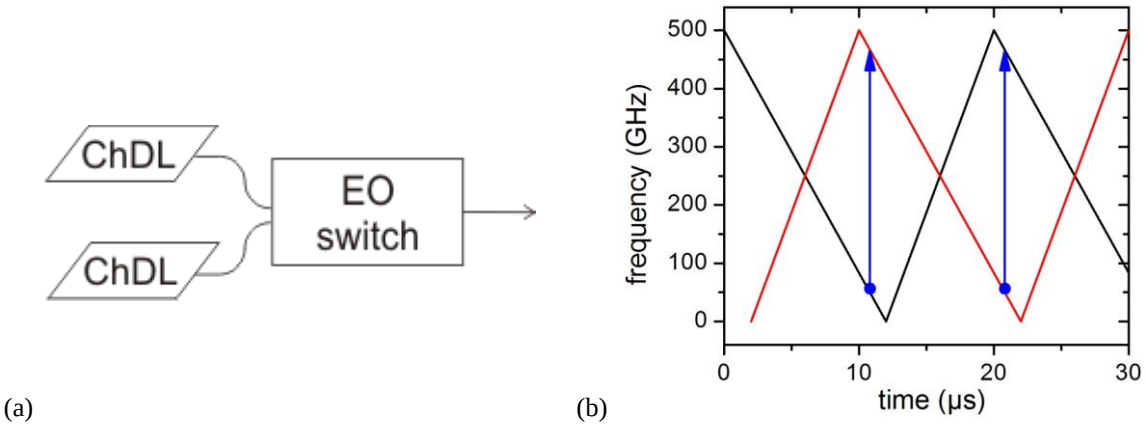

(a) (b)

Figure 12. (a) Dual source, consisting of two synchronized, out of phase chirped diode lasers with a 2x1 electro-optic switch. (b) Frequency vs time waveform, showing the transitions (blue line) between source one (black line) to source two (red line).

The dual source was injected into a YbFA, with three photodiodes to monitor the power going into the final stage, the output power, and the backward power leaving the final stage (figure 13a). The final stage is 20/400 double clad fiber. The results shown in figure 13 were obtained with a negative sawtooth. For a negative-chirp sawtooth, the power entering the final stage has unintentional modulation (figure 13b, red trace) due to wavelength- and polarization-dependent loss/gain and dispersion in the components between the seed lasers and the the pre-amplifier, including the electro-optic switch and the taps. The output power (figure 13b, top black trace) has about the same amount of modulation. The backward SBS measured with a fast photodiode shows the pulses characteristic of the initiation from spontaneous scattering (bottom black trace).

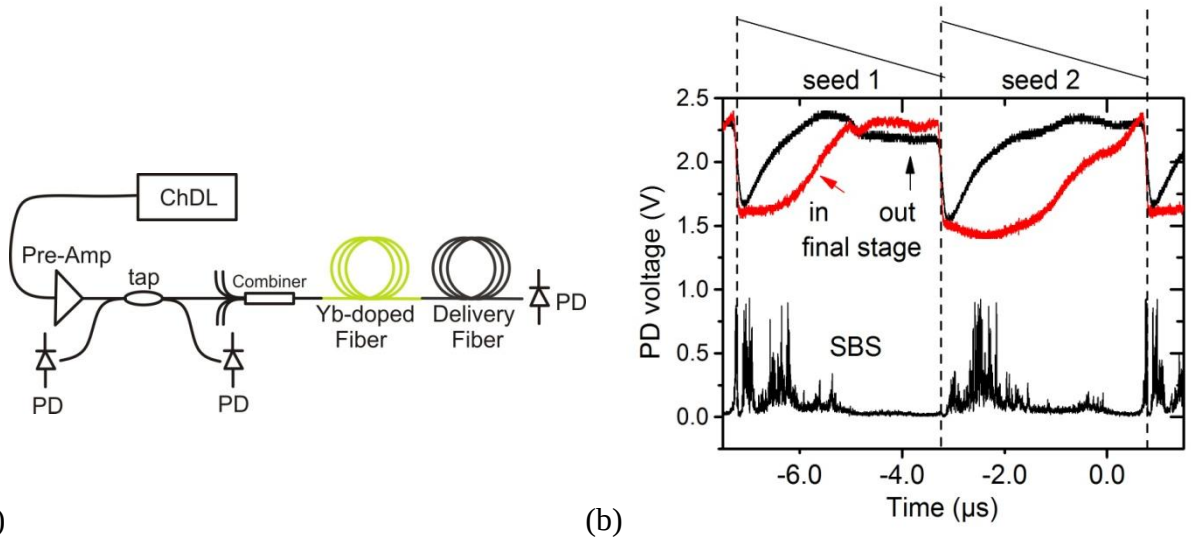

(a) (b)

Figure 13. Experimental apparatus for measuring input power to the final stage, backwards SBS power, and output power. (b) Oscilloscope traces from the three photodiodes taken at an output power of 600 W. The modulation on the input to the final stage is due to phase and amplitude dispersion in the pre-amplifier.

The backward SBS power was also measured with an averaging detector, and then plotted vs. the output power (figure 14a). The output power was varied by changing the current to the diodes pumping the final stage. The backward power clearly shows a threshold behavior. We define threshold as the point where the backward power equals 10^{-4} times the output power, and we can then plot the threshold output power vs. chirp (figure 14b). The threshold output power (black squares) is clearly increasing linearly with chirp, as shown by the dashed red line. Based on this, we expect the next generation of chirped diode lasers with a factor of 10 higher chirp to enable ~6 kW output powers. As shown in the next section, chirped seed amplifiers will also be coherently combinable.

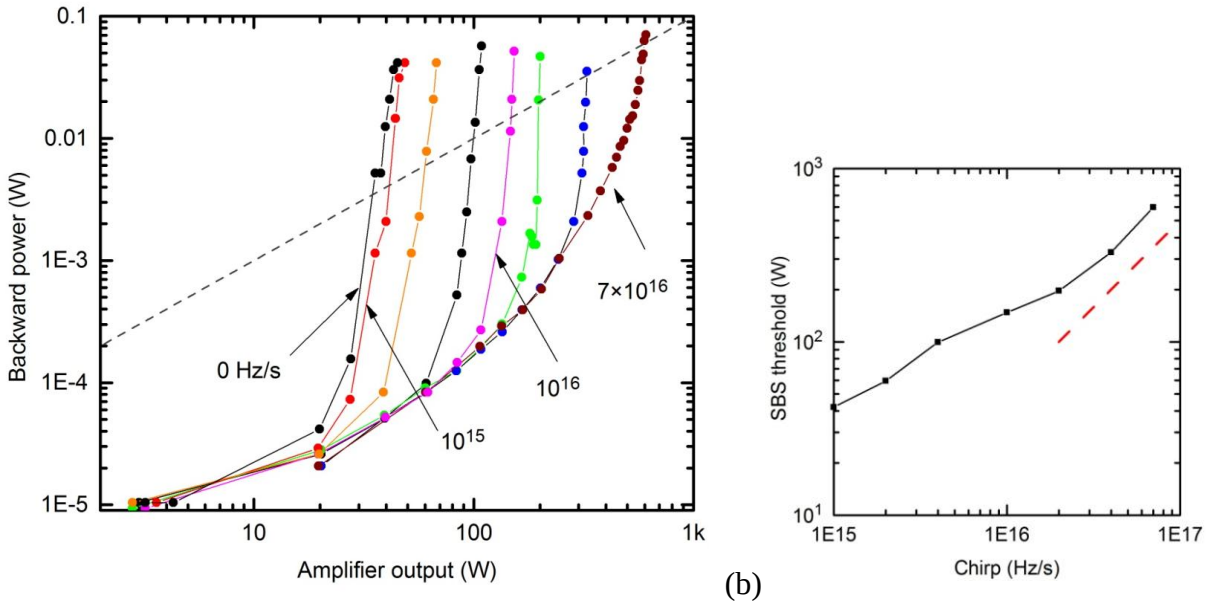

Figure 14. (a) Backward power from the final stage vs amplifier output power, for various chirps. The dashed line represents a backward power equal to 10^{-4} times the output power, used here to define SBS threshold. (b) SBS threshold vs chirp, as defined above. The dashed line represents a linear scaling of threshold with chirp.

6. Coherent Combining of Chirped Seed Yb Fiber Amplifier at 1.06 µm

Interference fringes were observed by overlapping the outputs of two 20-W Yb fiber amplifiers (figure 15a–d). The fringe visibility depends on many factors, in addition to the residual phase error of the feedback loop: the quality of the two wavefronts, how well the intensity profiles match, and whether the polarizations are parallel. The residual phase error can be estimated via an I/Q demodulation of the signal coming from the photodiode in the feedback loop (figure 15e). For the case of a chirp equal to 2.4×10^{14} Hz/s and a path length mismatch of 1.7 cm, the residual phase error is 0.15 rad, ignoring the transient at $t = 2s$ between sweeps. This leads to a theoretical coherent combining efficiency of $\eta = 98.9\%$. For a mismatch of 39 cm, the residual phase error was 0.42 rad, i.e. $\eta = 91.2\%$.

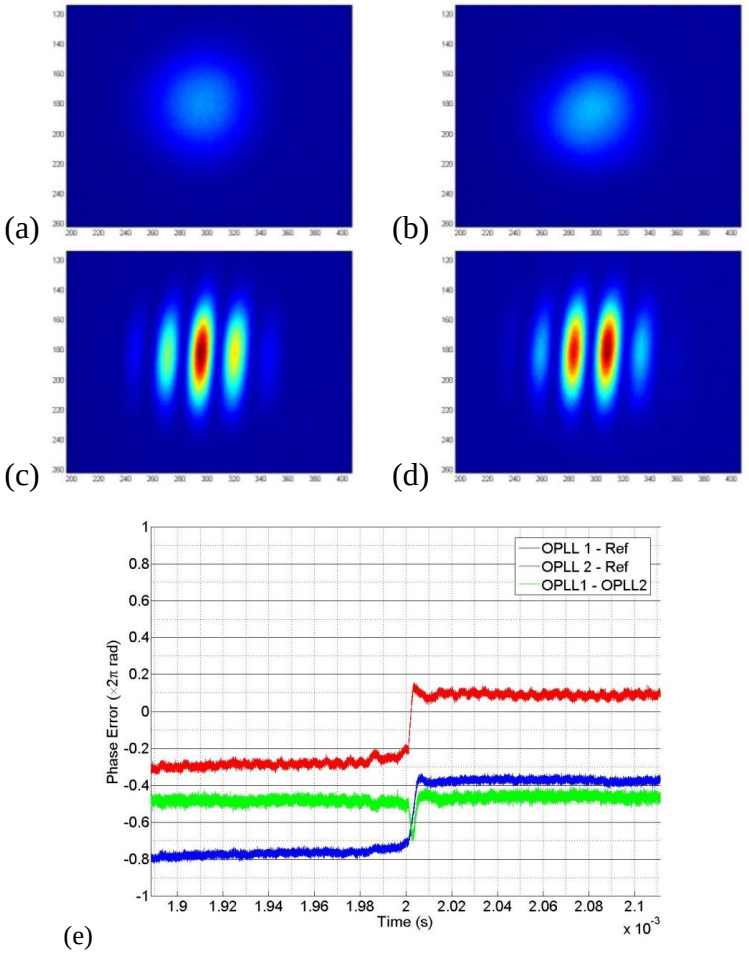

Figure 15. Intensity profiles of the beams exiting a two-channel Yb fiber amplifier; each channel emitting 20 W. (a) Channel A alone, (b) channel B, (c) both channels present and in phase, (d) out of phase. (e) The top (red) trace is the phase of channel A relative to the reference, as obtained by I/Q demodulation. The bottom (blue) trace is the phase of channel B relative to the reference. The middle (green) curve is the relative phase of channels A and B.

7. Multi-Mode Instability Suppression

For applications that require high spatial brightness, another bottleneck in the scaling of large mode area fiber lasers is the multimode instability that occurs at high-average-power. It is generally attributed to either (a) transverse spatial hole burning, or (b) a coupling between modes created when their interference gives rise to a spatially periodic variation of the gain or index in the core along the longitudinal direction. The analysis in this section shows that the problem of a coupling between the LP_{01} and LP_{11} modes can be avoided with a chirped seed.

The effective index as a function of $V = k\ a\ NA$ is shown in figure 16a for the LP_{01} and LP_{11} modes in a typical LMA fiber. V is varied by changing the optical frequency; the fiber parameters ($NA = 0.06$ and core diameter $2a = 20$ μ) are fixed. The vertical dashed line indicates $V = 3.56$ associated with a wavelength of 1.06 μ. The wavevector of the grating formed between the two modes is shown in figure 16b. At 1.06 μ, the grating vector $g \cong 2.87 \times 10^3$ m^{-1}, i.e., the grating period $\Lambda \cong 0.35$ mm. Because the slope of $g(V)$ is non-zero, the grating vector will change as the seed sweeps in frequency. For frequency sweeps of a few percent, the change Δg that occurs during a sweep $\Delta\nu = \nu_1 - \nu_2$ can be approximated by $\Delta g = (dg/d\nu)\Delta\nu$ (figure 16c).

Higher order modes in the final stage amplifier—e.g., the LP_{11} mode—are typically excited at the splice between a single-mode fiber and the LMA fiber. If the relative phase between the two modes is fixed at the splice, the grating will expand or contract from that point. At a distance $L_\pi = \pi/\Delta g$ from the splice, the spatial interference when the seed is at ν_1 and at ν_2 will be π out of phase. L_π is shown in figure 16d as a function of wavelength, for frequency sweeps of 0.5, 1.0, and 2.0 THz.

If the seed sweep time is short compared to the thermal diffusion time, any thermally induced change in gain or index will be washed out after a distance L_π. Because the grating period is an order of magnitude larger than the core diameter, the relevant diffusion time is $\tau = a^2\rho C/\kappa$, where ρ is the density, C is the specific heat, and κ is the thermal conductivity. For a 20 μ fused silica core, $\tau = 0.11$ ms. For a 30 μ core diameter, $\tau = 0.25$ ms. In our system, the high chirps are obtained at sweep time of less than 0.1 ms, so the thermally induced grating should be negligible after a distance L_π from the splice.

If the seed tunes over a range of 2 THz (8 nm at 1.06 μ), $L_\pi \cong 0.5$ m (figure 16d). For a 10 m active fiber, this could represent an order of magnitude increase in the threshold for multimode instability.

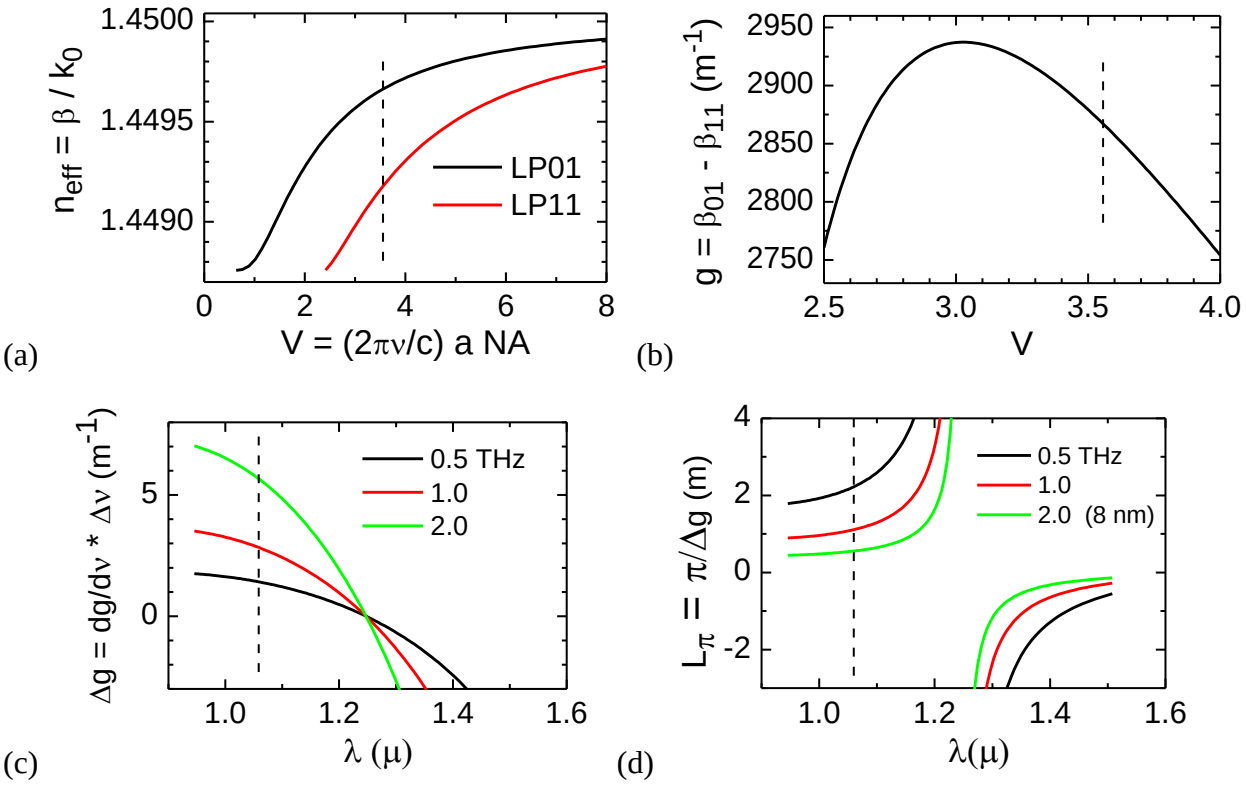

Figure 16. (a) Effective index as a function of the V number (normalized frequency) for the two lowest order modes of a step index fiber. Fiber frequency for the two lowest order modes in a step index LMA fiber (NA=0.06 and core diameter $2a = 20$ μ). (b) The wavevector of the grating formed by the interference of the two modes. (c) The change in grating vector for sweeps of 0.5–2.0 THz. (d) L_π as a function of wavelength, for sweeps of 0.5–2.0 THz.

8. Conclusions

Chirped seed amplification has been shown experimentally to raise the threshold for stimulated Brillouin scattering in a Yb fiber amplifier. For a chirp of 7×10^{16} Hz/s, the SBS threshold was raised to 600 W, compared to a threshold of 40 W at zero chirp. Furthermore, we demonstrated that the threshold scales linearly with chirp, so that a chirp of 5×10^{17} Hz/s, for example, should enable a 4 kW coherently combinable fiber amplifier. The next generation of chirped seed lasers will use MEMS-VCSELs (*15, 16*), which can tune up to 10^{18} Hz/s. Whether the tuning can be made linear enough for coherent combining is the subject of the next contract.

A unique feature of this seed is that the bandwidth, as seen by the counter-propagating SBS, increases linearly with delivery fiber length, so that the threshold decreases slower than 1/L. Enabling long delivery fibers is very important for integrating lasers into trucks, ships, and airplanes. One needs the flexibility to position the laser and the exit aperture in different locations. Lastly, the large mode-hop-free tuning range available from vertical cavity surface

emitting lasers also provides a path to suppressing multimode instability, another bottleneck in the scaling of high power fiber lasers.

9. References

1. Nufern (E. Granby, CT), Lockheed Martin (Bothell, WA), IPG Photonics (Oxford, MA).
2. Fan, T. Y.; Sanchez, A Coherent (Phased Array) and Wavelength (Spectral) Beam Combining Compared. *Proc. SPIE* **2005**, 5709, 157-164.
3. White, J. O.; Vasilyev, A.; Cahill, J. P.; Satyan, N.; Okusaga, O.; Rakuljic, G.; Mungan, C. E.; Yariv, A. Suppression of Stimulated Brillouin Scattering in Optical Fibers Using a Linearly Chirped Diode Laser. *Optics Express* **2012**, *20*, 15872–15881.
4. Lanticq, V.; Jiang, S.; Gabet, R.; Jaouën, Y.; Taillade, F.; Moreau, G.; Agarwal, G. P. Self-Referenced and Single-Ended Method to Measure Brillouin Gain in Monomode Optical Fibers. *Opt. Lett.* **2009**, *34*, 1018.
5. Satyan, N.; Vasilyev, A.; Rakuljic, G.; Leyva, V.; Yariv, A. Precise Control of Broadband Frequency Chirps Using Optoelectronic Feedback. *Opt. Express* **2009**, *17*, 15991.
6. Mungan, C. E.; Rogers, S. D.; Satyan, N.; White, J. O. Time-Dependent Modeling of Brillouin Scattering in Optical Fibers Excited by a Chirped Diode Laser. *IEEE J. Quantum Elect.* **2012**, *48*, 1542–1546.
7. Engin, D. Fibertek, Inc.
8. Goodno, G. D.; McNaught, S. J.; Rothenberg, J. E.; McComb, T. S.; Thielen, P. A.; Wickham, M. G.; Weber, M. E. Active Phase and Polarization Locking of a 1.4 kW Fiber Amplifier. *Opt. Lett.* **2010**, *35*, 1542–1544.
9. Satyan, N.; Vasilyev, A.; Rakuljic, G.; White, Jeffrey O.; Yariv, A. Phase-Locking and Coherent Power Combining of Broadband Linearly Chirped Optical Waves. *Optics Express* **2012**, *20*, 25213.
10. Model AMF100-10, Brimrose Corp., Baltimore, MD.
11. Vasilyev, A.; Petersen, E.; Satyan, N.; Rakuljic, G.; Yariv, A.; White, J. O. Coherent Power Combining of Chirped Seed Erbium-Doped Fiber Amplifiers. *IEEE Photonics Technology Lett.* **2013**, *25*, 1616–1618.
12. Petersen, E.; Yang, Z. Y.; Satyan, N.; Vasilyev, A.; Rakuljic, G.; Yariv, A.; White, J. O. *IEEE J. Quantum Elect.* **2013**, *49*, 1040–1045.
13. Model SLD1050P, Thorlabs, Newton, NJ.
14. Model NSSW-121115323, www.agiltron.com Agiltron, Wilmington, MA.

15. Jayaraman, V.; Cole, G. D.; Robertson, M.; Burgner, C.; John, D.; Uddin, A.; Cable, A. Rapidly Swept, Ultra-Widely-Tunable 1060 nm. *MEMS-VCSELs Electronics Letters* **2012**, *48*, 1331.

16. Chase, C.; Rao, Y.; Hofmann, W.; Chang-Hasnain, C. 1550 nm High Contrast Grating. *VCSEL Optics Express* **2010**, *18*, 15461.

NO. OF COPIES	ORGANIZATION
1 (PDF)	DEFENSE TECHNICAL INFORMATION CTR DTIC OCA
2 (PDFS)	DIRECTOR US ARMY RESEARCH LAB RDRL CIO LL IMAL HRA MAIL & RECORDS MGMT
1 (PDF)	GOVT PRINTG OFC A MALHOTRA
1 (PDF)	DIRECTOR HEL-JTO LARRY GRIMES
1 (PDF)	ASSISTANT DIRECTOR HEL-JTO DON SEELEY
1 (PDF)	HEL-JTO WALTER FINK
1 (PDF)	SCHAFER ASSOCIATES JACK SLATER
1 (PDF)	DARPA JOSEPH MANGANO
1 (PDF)	USNA CARL MUNGAN
1 (PDF)	MIT LINCOLN LABS DAN RIPIN
3 (PDFS)	DIRECTOR US ARMY RESEARCH LAB RDRL SEE GARY WOOD RDRL SEE M LARRY STOUT JEFFREY O. WHITE

INTENTIONALLY LEFT BLANK.